JCI insight

Rapamycin and dexamethasone during pregnancy prevents tuberous sclerosis complex associated cystic kidney disease

Morris Nechama, Yaniv Makayes, Elad Resnick, Karen Meir, Oded Volovelsky

JCI Insight. 2020. https://doi.org/10.1172/jci.insight.136857.

Research In-Press Preview Nephrology

Graphical abstract

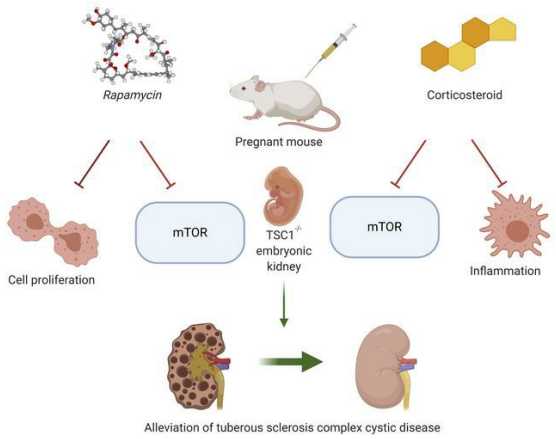

Rapamycin and dexamethasone during pregnancy prevents tuberous sclerosis complex associated cystic kidney disease

Morris Nechama[1], Yaniv Makayes[1], Elad Resnick[1], Karen Meir[2], Oded Volovelsky[1]

[1]Pediatric Nephrology Unit, Hadassah-Hebrew University Medical Center, Jerusalem, Israel
[2]Department of Pathology, Hadassah-Hebrew University Medical Center, Jerusalem, Israel

Address correspondence to: Oded Volovelsky, Pediatric Nephrology Unit, Hadassah-Hebrew University Medical Center, Ein-Kerem Campus, Jerusalem, 91120, POB 12000, Israel, +972-2-6777023, [odedvo@hadassah.org.il].

Conflict of interest statement: The authors have declared that no conflict of interest exists.

Abstract

Chronic kidney disease is the main cause of mortality in patients with tuberous sclerosis complex disease (TSC). The mechanisms underlying TSC cystic kidney disease remain unclear with no available interventions to prevent cyst formation. Using targeted deletion of *TSC1* in nephron progenitor cells, we showed that cysts in *TSC1* null embryonic kidneys originate from injured proximal tubular cells with high mTOR complex 1 activity. Injection of rapamycin to pregnant mice inhibited the mTOR pathway and tubular cell proliferation in kidneys of *TSC1* null offspring. Rapamycin also prevented renal cystogenesis and prolonged the life span of TSC newborns. Gene expression analysis of proximal tubule cells, identified sets of genes and pathways that were modified secondary to *TSC1* deletion and rescued by rapamycin administration during nephrogenesis. Inflammation with mononuclear infiltration was observed in the cystic areas of *TSC1* null kidneys. Dexamethasone administration during pregnancy decreased cyst formation not only by inhibiting the inflammatory response but also by interfering with the mTORC1 pathway. These results reveal novel mechanisms of cystogenesis in TSC disease and suggest new interventions prior to birth to ameliorate cystic disease in offspring.

Introduction

Tuberous sclerosis complex disease (TSC) is a genetic disorder affecting various organs, including the brain, kidney, skin, and heart, with an estimated prevalence of approximately 1:6,000 in all populations studied (1-4). De novo or inherited autosomal dominant mutations in *TSC1* or *TSC2* result in inactivation of tuberous sclerosis complex composed of hamartin and tuberin proteins, respectively. The complex acts as a tumor suppressor and inhibits the activity of mTOR complex 1 (mTORC1), a central regulator of various cellular functions such as protein translation, proliferation, metabolism, and autophagy (5-7). However, the hamartin-tuberin complex also has mTORC1 independent cellular effects through distinct pathways. For instance, we have previously shown that the effect of improved nephron endowment by TSC1 hemizygous deletion in nephron progenitor cells (NPCs) is independent of mTORC1 activity (8, 9). Interruption of the hamartin-tuberin complex by *TSC2* deletion also has mTORC1 independent effects on prostaglandin production and NOTCH activity (10-12). PAK2 and TGFB-Smad2/3 signaling pathways were suggested to mediate this independent effect as well (13, 14). Moreover, in cancer cells, *TSC2* was shown to regulate VEGF gene expression in a mTOR independent pathway (15). Indeed, some of the clinical manifestations of TSC disease respond only partially to mTOR inhibitors (2, 13, 14, 16, 17).

TSC has debilitating neurological effects in childhood, including convulsions and autism spectrum disorder, which usually stabilize in late adolescence (18, 19). Chronic kidney disease (CKD) is the main cause of morbidity in adult TSC patients (20, 21). The renal manifestations of TSC include renal angiomyolipoma (AML), benign vascular lesions, and cystic disease of the kidneys, which appear in the majority of patients (21, 22). AML of large dimensions poses an increased risk of bleeding if left untreated. Cystic kidney disease leads to a gradual loss of renal parenchyma, aggravated by the decline in nephron number consequent to multiple surgical procedures for AML resections and ablations. As a result, TSC patients are exposed to complications of CKD at an earlier age than the general population. About 40% of TSC patients eventually develop advanced CKD (stage

III-V) (23). The burden of CKD in TSC patients ranges in severity from a single renal cyst to a severe polycystic phenotype, especially in of *TSC2* and *PKD1* (24, 25). The precise pathomechanism by which this autosomal dominant disorder causes cystic renal disease remains poorly understood. Furthermore, while mTOR inhibitors reduce the size and bleeding risk of large AML (16, 26), their therapeutic effects, and even more critical, their preventive effects on TSC cystic kidney disease, are still controversial (21, 27, 28).

We previously generated a mouse model of TSC by specific deletion of *TSC1* in NPCs using Cre-Lox recombination in mice (8). NPCs differentiate into the various segments of the nephron, forming the basic filtering unit. They originate from the embryonic metanephric mesenchyme and disappear in the third postpartum day in mice, with no subsequent regeneration. While *TSC1* hemizygous deletion induces nephrogenesis, complete deletion of *TSC1* leads to a lethal cystic phenotype characterized by severe injury to the renal proximal tubular cells (PTCs) (8).

We now show that mononuclear inflammation, especially macrophage infiltration, plays a central role in cystogenesis in CKD of TSC. The cyst formation is paralleled by increased mTOR activity and cystogenic processes, such as increased c-Myc expression and cell proliferation. Furthermore, the cystic disease in offspring can be prevented using mTOR inhibitors and corticosteroids during pregnancy. Our findings identify new mechanisms and therapeutic targets to overcome TSC cystic kidney disease.

Results

We previously showed that complete deletion of *TSC1* in NPCs induces tubular damage as early as E15.5 with swollen cellular appearance and occluded lumen and cyst formation was evident at E17.5 (Figure 1A-B) (8). Dissection of kidneys from *TSC1* null embryos at various time points during embryogenesis herein identified increased phosphorylation of ribosomal protein S6 (pS6), the main downstream target of mTORC1 at E15.5 and E17.5 (Figure 1C). The increased levels of pS6 were evident in the damaged PTCs as was determined by LTL (Lotus Tetragonolobus Lectin) positive cyst lining epithelial cells (Figure 1D, Supplementary Figure 1). The cysts appear in the late stages of pregnancy, beginning at E17.5. Therefore, the increased pS6 staining appears initially in the injured tubular cells and then in the cyst lining epithelial cells originates from the proximal tubular cells. Therefore, TSC1 deletion in NPCs leads to proximal tubular injury and cyst formation, associated with mTORC1 activation.

Next, we examined whether mTORC1 inhibition alleviates TSC tubular damage and cystogenesis. $TSC1^{f/f}$ female mice were mated with *Six2* $Cre^{tg/+}$ $TSC1^{f/+}$ males to generate *Six2* $Cre^{tg/+}$ $TSC1^{f/f}$ pups with NPC-specific TSC deletion (25% of offspring). Pregnant $TSC1^{f/f}$ females were injected with rapamycin, a potent and specific inhibitor of mTORC1 or vehicle, on embryonic days E12.5, E14.5, and E16.5 (Figure 2A). We measured tubular damage and cyst formation in kidneys of the $TSC1^{-/-}$ offspring. Rapamycin prevented cellular injury and cystogenesis, as demonstrated by a decline in cyst area and number (Figure 2B and C). While mTOR activity was dramatically increased in $TSC1^{-/-}$ compared to control littermates, rapamycin decreased mTORC1 activity, as was shown by reduced pS6 levels in both null and hemizygous *TSC1* kidneys compared to controls. pS6 levels were decreased by both immunofluorescent (IF) staining and Western blot analysis (Figure 2B, D-E, Supplementary Figure 3).

c-Myc is a potent transcription factor involved in diverse cellular activities, previously demonstrated to be involved in cystogenesis in autosomal dominant polycystic kidney disease

(ADPKD) (29, 30). In addition to the increase in mTORC1 activity, c-Myc levels were increased in both hemizygous and *TSC1* null kidneys. Furthermore, c-Myc was predominantly expressed in cyst lining epithelial cells (Figure 2B). Rapamycin decreased c-Myc levels as observed by both IF staining and Western blot analysis (Figure 2B, 2D-E). Cell proliferation was also inhibited by rapamycin, as measured by decreased expression of the proliferation marker Ki67. Therefore, rapamycin ameliorates cystic kidney disease by reducing mTOR activity, c-Myc expression, and cell proliferation, all of which have been previously shown to be involved in cyst formation in other renal cystic diseases (29, 30).

NPC specific *TSC1* null mice die two days after birth (8). We therefore investigated whether rapamycin improves the survival of TSC mice. To that end, we monitored the effect of rapamycin administered during pregnancy on offspring survival. Rapamycin prolonged the survival of pups up to the age of P14, demonstrating a significant effect of rapamycin after birth (Figure 2F). At P14, the effect of rapamycin was no longer evident, and the mice had a high cystic burden and increased pS6 expression in the proximal tubules due to *TSC1* ablation (Supplementary Figure 2). Thus, rapamycin administration during pregnancy prolongs the life span of newborn TSC mice by transient inhibition of renal tubular damage and cystogenesis.

We then examined the effect of *TSC1* deletion on global gene expression and intracellular pathways in PTCs and the impact of rapamycin on both. For this purpose, we sorted Prominin1 positive PTCs from control and *Six2 Cre$^{tg/+}$TSC1$^{f/f}$* mice (31), with and without rapamycin as above (Figure 2A and 3A). Gene expression was analyzed by RNA sequencing to identify genes and pathways that were affected by *TSC1* deletion and rescued by rapamycin treatment during pregnancy (Figure 3B). Among these pathways, we found an increase in the expression of genes related to inflammatory response and complement pathway activation in *TSC1* null mice PTCs compared to controls. The expression of these genes was downregulated in PTCs from pups of mothers injected

with rapamycin during pregnancy (Figure 3C-E). Many of these genes are associated with macrophage polarization and chemotaxis to the inflammation site (32-34).

Inflammation with high mononuclear cell infiltration was evident in cystic kidneys of *TSC1* null P14 mice (Figure 2G). Cystic kidneys of *TSC1* null P0 mice demonstrated increased levels of the NF-κB P65 subunit protein (Figure 4A-C). Increased macrophage infiltration in P0 mice was demonstrated also by high levels of the F4/80 macrophage marker expression by immunostaining, as well as high levels of $F4/80^{+}$ cells in dissociated $TSC1^{-/-}$ kidneys, as reflected by FACS analysis (Figure 4A, D). Therefore, cystic kidneys in TSC show an inflammatory response and macrophage infiltration.

We next examined whether anti-inflammatory treatment during pregnancy prevents the TSC cystic disease in a similar manner as mTOR inhibition. Corticosteroids are potent anti-inflammatory medications which are frequently used during high-risk preterm pregnancies for various indications, including acceleration of lung maturation (35). Dexamethasone was injected to pregnant TSC mice carrying *TSC1* null embryos, at the same time course as rapamycin (E12.5, E14.5, and E16.5) (Figure 2A). Dexamethasone administration during gestation improved renal cystic burden (Figure 4E, F) and significantly reduced macrophage infiltration as indicated by F4/80 immunostaining and FACS analysis (Figure 4E, G-H). However, dexamethasone did not rescue the injured proximal tubular morphology, as these still demonstrated swollen epithelial cells and occluded lumens. Dexamethasone decreased mTORC1 activity but not P65 in TSC cystic kidneys (Figure 4I-K). Therefore, inflammation plays a central role in the pathogenesis of cystic TSC kidney disease and corticosteroid administration during gestation prevents cystogenesis in TSC by inhibiting both mTOR activation and inflammation.

Discussion

In our TSC mouse model, *TSC1* deletion in NPCs induces proximal tubule cell damage and cyst formation, starting as early as E15.5. Based on our findings, mTORC1 hyperactivation in TSC null proximal renal tubules leads to tubular cell damage and proliferation, also through c-Myc activation. Administration of steroids during pregnancy prevents cyst formation in TSC offspring, not only by hindering the inflammatory process, as the high macrophage infiltration, but also by downregulating mTORC1 activity (Figure 5).

Various murine models were based on *TSC1* or *TSC2* deletions in distinct portions of the nephron. In the current model, elimination of the two *TSC1* alleles was introduced specifically in the progenitor cells, and therefore, it is present in most segments of the nephron in the offspring. Using this strategy, we also show that the resulting cysts originate from the proximal tubules. Moreover, the severe cystic disease appears only following homozygous deletion of *TSC1* in our model. It has been previously suggested that a second hit, which leads to loss of heterozygosity, takes place in the cystic cells as reported in TSC-angiomyolipoma and pulmonary lymphangiomatosis (LAM). However, the reports on loss of heterozygosity in TSC renal cysts are not consistent (36, 37).

Rapamycin has been successfully used during pregnancy in small clinical trials to prevent TSC manifestations, such as cardiac tumors (38, 39). Benefits from the early use of rapamycin were also demonstrated in neurological manifestations of TS, such as developmental delay (40). However, the safety of rapamycin during pregnancy has not been studied thoroughly in human studies and teratogenic effects have been reported in animal models (39, 41). Our findings suggest that the use of anti-inflammatory agents such as corticosteroids may reduce kidney damage induced by cystogenesis. Indeed, corticosteroids such as dexamethasone and betamethasone are commonly used during pregnancy and, therefore, may serve as an alternative approach for the treatment of TSC.

Previous studies demonstrated that the catabolic effect of glucocorticoids on skeletal muscle is also mediated by inhibition of the mTOR pathway. Steroid administration led to decreased levels

of phosphorylated 4EBP1 and S6 kinase 1, the main downstream targets of mTORC1. It has been suggested that glucocorticoids enhance the expression of REDD1, a mTORC1 suppressor (42-44). Our study is the first report of the effect of glucocorticoids on TSC disease, such as cystic kidney disease. We show that the effect of glucocorticoids is direct through modulation of mTORC1 activity, as well as by the inhibition of the inflammatory response which is essential for TSC cystogenesis (42-44).

Our results indicate increased c-Myc expression in TSC cystic epithelial cells that is mTOR dependent. A relationship between the hamartin-tuberin complex, acting as a tumor suppressor gene, and c-Myc has been studied in tumors (45-47). c-Myc, as a potent oncogene, induces expression of genes involved in cell proliferation in various tumors. On the one hand, c-Myc is a direct repressor of *TSC2* expression encoding tuberin, the co-protein of hamartin. On the other, loss of tuberous sclerosis complex by loss of tuberin, enhances the expression of c-Myc and thereby causes an oncogenic loop. The effect of loss of tuberous sclerosis complex is mediated by hyperactivation of mTORC1. mTORC1 is required for proper translation of c-Myc as well as its post transcriptional modification to enhance c-Myc stability (48). Lately, a similar relationship of c-Myc with hamartin encoded by *TSC1* was revealed in c-Myc driven tumors such as Burkitt's lymphoma, also in a mTORC1 dependent manner (46). Indeed, renal cystogenesis is characterized by an increased proliferation rate of tubular cells. Analysis of ADPKD kidney biopsies also confirmed increased c-Myc expression specifically in the cystic epithelial cells concurrent with an increased proliferation rate (29, 30, 49, 50). Inhibition of c-Myc significantly reduced cystogenesis in vivo (51). Here, we report that interruption of hamartin-tuberin complex in NPCs by *TSC1* deletion during pregnancy is associated with high c-Myc activity and proliferation rate in TSC cyst lining cells.

The role of inflammation in TSC manifestation was also demonstrated in TSC related tumors. Rapamycin leads to only partial regression of TSC tumors, including AML, with a high risk of relapse of the tumor after cessation of rapamycin therapy. The adequate response of the immune system to

the tumors may also be impaired by the effect of rapamycin on the immune system. Immunotherapy by PD-1 and CTLA-4 blockade leads to substantial regression of TSC related tumors with long-term remission, which may be further improved by combination therapy with mTORC1 inhibitors (52-57).

Our findings on the role of inflammation in TSC cystic disease are compatible with new evidence demonstrating that macrophages play a central role in cyst formation and progression in ADPKD (58, 59). Previous studies have shown that infiltrating macrophages are initially of the pro-inflammatory classically activated M1-like type, which exacerbate tubular injury due to their release of reactive oxygen and nitrogen intermediates (60). Later, the M1-like macrophages are converted to alternatively activated M2-like macrophages, which then stimulate the proliferation of tubular epithelial cells for the apparent purpose of facilitating the repair of the sustained injury. Whether the same molecular mechanisms by which macrophages induce cytogenesis in ADPKD are activated in TSC, awaits further investigation.

We demonstrate that hyperactivation of mTOR plays a central role in TSC cystic kidney disease by increasing PTC proliferation rate which is mediated also by enhancing c-Myc activity. We also show that increased inflammation, mainly macrophagic infiltration contributes to cyst formation in TSC, as demonstrated in other cystic kidney disease. Steroid administration diminishes cystogenesis not only by modulating the inflammatory response but also by interfering with mTORC1 activity, as has been demonstrated in other organs. Our findings raise a new alternative strategy for early intervention during pregnancy to prevent long-term kidney disease as a result of cyst formation in TSC. Our data may also contribute to the understanding of other aspects of TSC disease, such as AML, in the kidney as well as in other organs.

Methods

Animals

All mice were maintained in the Hebrew University Specific-Pathogen-Free (SPF) Animal Facility Unit. The transgenic mice were a gift from Raphael Kopan's lab from the division of developmental biology from Cincinnati children's hospital medical center. The following CD1 transgenic mice lines were used: *Tg(Six2-EGFP/cre)1Amc* (herein *Six2Cre$^{tg/+}$*) and *TSC1$^{f/f}$* (8). For heterozygous deletion of *TSC1* in NPCs, 6-8 week old *Six2Cre$^{tg/+}$* male mice were mated with 6-8 week old *TSC1$^{f/f}$* females. To generate homozygous *TSC1* deletion (*Six2Cre$^{tg/+}$ TSC1$^{f/f}$*) mice, 6-8 week old heterozygous *Six2Cre$^{tg/+}$ TSC1$^{f/+}$* males were backcrossed with 6-8 week old *TSC1$^{f/f}$* females. The pregnancy date was determined by vaginal plug expulsion. The morning of plug detection was designated as day 0.5 of pregnancy. At different embryonic dates, pregnant females were sacrificed using CO_2 and cervical dislocation. The embryos and newborn pups were dissected, and kidneys were excised for histopathology evaluation. In some experiments, Rapamycin (0.2 mg/kg), Dexamethasone (0.1 mg/kg) or vehicle (DMSO or PBS respectively) were intraperitoneally injected.

Histology

Embryonic or newborn mouse kidneys were dissected on ice-cold PBS and fixed overnight in fresh 4% formaldehyde in PBS. Kidneys were embedded in paraffin for sectioning. For overall histology, tissue sections were stained with hematoxylin/eosin and PAS staining. Immunohistochemistry (IHC) and IF staining were performed as previously described (8, 61). Briefly, paraffin-embedded tissue sections (4–6 μm) were deparaffinized, hydrated and incubated overnight at 4° C with the following reagents, according to the manufacturer's instructions; Biotin anti-LTL (B-1325, VECTOR laboratories), rabbit anti-phospho S6 ribosomal protein (2211, Cell Signaling Technology), mouse anti-c-Myc (Sc-40, Santa Cruz Biotechnology Inc), rabbit anti Ki-67 (MU297-UC, Biogenex), rabbit anti P65 (8242, Cell Signaling Technology), rat anti F4/80 (MCA497, Bio-Rad). For IHC, DAB

reagent was applied after incubation with the appropriate HRP-bound secondary antibody. For IF staining, the sections were incubated with either Cy3 conjugated goat anti-rabbit or Cy5 conjugated goat anti-mouse antibody, according to the manufacturer's instruction (Jackson Immuno Research Laboratories). The sections were visualized with a confocal A1R microscope at 20× magnification unless stated otherwise.

Cystic index

The cyst number for a given section area and the cyst area ratio compared to total kidney section area, were evaluated with ImageJ analysis software.

Western blotting

Kidneys were extracted and homogenized in cold RIPA buffer containing 150 mM NaCl, 1% NP40, 0.5% sodium deoxycholate, 0.1% SDS, 25 mM Tris (pH 7.4), supplemented with protease/phosphatase inhibitors (4906837001, MERCK). An equal amount of protein extract was analyzed by SDS-PAGE as previously described (61) using the following antibodies as above, according to the manufacturer instructions, rabbit anti-phospho-S6 ribosomal protein, mouse anti-c-Myc (Sc-40, Santa Cruz Biotechnology Inc.), rabbit anti P65 (8242, Cell Signaling Technology) and mouse anti GAPDH (MAB374, EMD Millipore).

Fluorescence-activated cell sorting (FACS) of proximal tubular cells

Kidneys were excised in ice-cold HBSS buffer. The kidneys were sliced and chopped into ~0.5-1 mm pieces on ice using a surgical scalpel. The chopped kidneys were transferred into HBSS solution containing 1 μg/μl collagenase/Dispase (10269638001, Sigma Aldrich) and incubated for 25 minutes at 37^0 C. The cells were filtered through a 40 μm nylon cell strainer (Corning) and washed twice with cold HBSS. For proximal tubular cell isolation, the cells were stained with PE-conjugated anti-CD133/prominin-1 antibody (12-1331-82, Invitrogen) according to manufacturer's instructions. PE^+ cells were isolated by cell flow cytometry-based cell sorting (Hebrew University Faculty of Medicine

Core Facility). The cells were washed and total RNA extracted using peqGOLD TriFast (PeqLab Biotechnologie). For FACS analysis of F4/80^{+} cells, kidneys were chopped as above and stained with APC conjugated anti F4/80 antibody (130-117-509, Macs Miltenyi Biotech). The cells were washed twice with HBSS before analysis by LSRII flow cytometry.

RNA sequencing and pathway analysis

The RNA quality was evaluated in TapeStation, using RNA ScreenTape kit (Agilent Technologies), and quantified using a Qubit apparatus (Qubit® DNA HS Assay kit, Invitrogen). Libraries were prepared from RNA samples using a KAPA Stranded mRNA-Seq Kit (KK8401, Roche). The libraries were barcoded and pooled for multiplex sequencing (1.5 pM total, including 1.5% PhiX control library). The pooled cDNA was loaded on NextSeq 500 High Output v2 kit (75 cycles) cartridge (Illumina) and sequenced on Illumina NextSeq 500 System, using sequencing conditions of 75 cycles, single-read. Library preparation and sequencing were performed at the Core Facility of the Hebrew University Faculty of Medicine. The RNA sequencing data have been deposited in NCBI's Gene Expression Omnibus, and are accessible under the accession code GSE152165. For further validation, RNA was extracted and used for qRT-PCR with the following primers: IL6 forward: 5'-CTCTGCAAGAGACTTCCATCCA-3'. IL6 reverse: 5'-GACAGGTCTGTTGGGAGTGG-3'. TNFA forward: 5'-TAGCCCACGTCGTAGCAAAC-3'. TNFA reverse: 5'-ACAAGGTACAACCCATCGGC-3'. CXCL10 forward: 5'-ATGACGGGCCAGTGAGAATG-3. CXCL10 reverse: 5'-TCGTGGCAATGATCTCAACAC-3'. CCL4 forward: 5'-CTGTGCAAACCTAACCCCGA-3'. CCL4 reverse: 5'-AGGGTCAGAGCCCATTGGT-3'.

Gene set enrichment analysis

Differential expression data from *TSC1*-KO versus *TSC1*-KO-Rapa were subjected to gene set enrichment analysis (GSEA, Broad Institute). GSEA uses ranked differential expression data (cut-off independent) to determine whether a priori–defined sets of genes show statistically significant and

concordant differences between two biological states. GSEA was run against the hallmark gene sets collection from the molecular signatures database (MSigDB).

Statistical analysis

The number of the biological samples were determined based on effect size or sample variation. No statistical method was used to predetermine the sample size. No animals or samples were excluded from any analysis. Animals were randomly assigned to groups for *in vivo* studies; no formal randomization method was applied when assigning animals for treatment. Values are reported as means ± standard error of the mean (SEM) unless otherwise stated. The data were analyzed by a Student's two-tailed *t*-test. In experiments as indicated one-way ANOVA analysis was performed followed by Duncan's post-hoc test. The significance was set at a p-value of <0.05. The data are presented using the GraphPad Prism version 7.

All animal studies were carried out in compliance with the ethical regulations approved by the Animal Care Committee of the Hebrew University Medical School (Ethical Approval Number: MD-17-15368-4).

Authors' contributions

MN and OV conceived the study, designed the experiment and wrote the manuscript. MN conducted most of the experiments and supervised the rest of the experiments. YM and ER conducted some of the experiments. KM helped to conceive the study and critically reviewed the manuscript.

Acknowledgments

This work was supported by grants from the Israel Science Foundation (to OV, 2358/18) and institutional grants (startup and bridging) from the Hadassah-Hebrew University Medical Center (to OV). OV and MN are research associates of the Wohl's Translation Research Institute at Hadassah-Hebrew University Medical Center. The graphical abstract was created with Biorender.com.

References

1. Osborne JP, Fryer A, and Webb D. Epidemiology of tuberous sclerosis. *Ann N Y Acad Sci.* 1991;615:125-7.
2. Crino PB, Nathanson KL, and Henske EP. The tuberous sclerosis complex. *N Engl J Med.* 2006;355(13):1345-56.
3. Yates JR. Tuberous sclerosis. *Eur J Hum Genet.* 2006;14(10):1065-73.
4. Hong CH, Tu HP, Lin JR, and Lee CH. An estimation of the incidence of tuberous sclerosis complex in a nationwide retrospective cohort study (1997-2010). *Br J Dermatol.* 2016;174(6):1282-9.
5. Consortium ECTS. Identification and characterization of the tuberous sclerosis gene on chromosome 16. *Cell.* 1993;75(7):1305-15.
6. van Slegtenhorst M, de Hoogt R, Hermans C, Nellist M, Janssen B, Verhoef S, et al. Identification of the tuberous sclerosis gene TSC1 on chromosome 9q34. *Science.* 1997;277(5327):805-8.
7. Dabora SL, Jozwiak S, Franz DN, Roberts PS, Nieto A, Chung J, et al. Mutational analysis in a cohort of 224 tuberous sclerosis patients indicates increased severity of TSC2, compared with TSC1, disease in multiple organs. *Am J Hum Genet.* 2001;68(1):64-80.
8. Volovelsky O, Nguyen T, Jarmas AE, Combes AN, Wilson SB, Little MH, et al. Hamartin regulates cessation of mouse nephrogenesis independently of Mtor. *Proc Natl Acad Sci U S A.* 2018;115(23):5998-6003.
9. Ingelfinger JR. Tackling Tsc1 to Promote Nephrogenesis. *N Engl J Med.* 2018;379(25):2476-8.
10. Hartman TR, Liu D, Zilfou JT, Robb V, Morrison T, Watnick T, et al. The tuberous sclerosis proteins regulate formation of the primary cilium via a rapamycin-insensitive and polycystin 1-independent pathway. *Hum Mol Genet.* 2009;18(1):151-63.
11. Karbowniczek M, Zitserman D, Khabibullin D, Hartman T, Yu J, Morrison T, et al. The evolutionarily conserved TSC/Rheb pathway activates Notch in tuberous sclerosis complex and Drosophila external sensory organ development. *J Clin Invest.* 2010;120(1):93-102.
12. Li C, Liu X, Liu Y, Zhang E, Medepalli K, Masuda K, et al. Tuberin Regulates Prostaglandin Receptor-Mediated Viability, via Rheb, in mTORC1-Hyperactive Cells. *Mol Cancer Res.* 2017;15(10):1318-30.

13. Alves MM, Fuhler GM, Queiroz KC, Scholma J, Goorden S, Anink J, et al. PAK2 is an effector of TSC1/2 signaling independent of mTOR and a potential therapeutic target for Tuberous Sclerosis Complex. *Sci Rep.* 2015;5:14534.
14. Thien A, Prentzell MT, Holzwarth B, Klasener K, Kuper I, Boehlke C, et al. TSC1 activates TGF-beta-Smad2/3 signaling in growth arrest and epithelial-to-mesenchymal transition. *Dev Cell.* 2015;32(5):617-30.
15. Brugarolas JB, Vazquez F, Reddy A, Sellers WR, and Kaelin WG. TSC2 regulates VEGF through mTOR-dependent and -independent pathways. *Cancer Cell.* 2003;4(2):147-58.
16. Bissler JJ, McCormack FX, Young LR, Elwing JM, Chuck G, Leonard JM, et al. Sirolimus for angiomyolipoma in tuberous sclerosis complex or lymphangioleiomyomatosis. *N Engl J Med.* 2008;358(2):140-51.
17. Yalon M, Ben-Sira L, Constantini S, and Toren A. Regression of subependymal giant cell astrocytomas with RAD001 (Everolimus) in tuberous sclerosis complex. *Childs Nerv Syst.* 2011;27(1):179-81.
18. Kingswood C, Bolton P, Crawford P, Harland C, Johnson SR, Sampson JR, et al. The clinical profile of tuberous sclerosis complex (TSC) in the United Kingdom: A retrospective cohort study in the Clinical Practice Research Datalink (CPRD). *Eur J Paediatr Neurol.* 2016;20(2):296-308.
19. Kingswood JC, d'Augères GB, Belousova E, Ferreira JC, Carter T, Castellana R, et al. TuberOus SClerosis registry to increase disease Awareness (TOSCA) - baseline data on 2093 patients. *Orphanet J Rare Dis.* 2017;12(1):2.
20. Shepherd CW, Gomez MR, Lie JT, and Crowson CS. Causes of death in patients with tuberous sclerosis. *Mayo Clin Proc.* 1991;66(8):792-6.
21. Dixon BP, Hulbert JC, and Bissler JJ. Tuberous sclerosis complex renal disease. *Nephron Exp Nephrol.* 2011;118(1):e15-20.
22. Siroky BJ, Yin H, and Bissler JJ. Clinical and molecular insights into tuberous sclerosis complex renal disease. *Pediatr Nephrol.* 2011;26(6):839-52.
23. Kingswood JC, Bissler JJ, Budde K, Hulbert J, Guay-Woodford L, Sampson JR, et al. Review of the Tuberous Sclerosis Renal Guidelines from the 2012 Consensus Conference: Current Data and Future Study. *Nephron.* 2016;134(2):51-8.
24. Sampson JR, Maheshwar MM, Aspinwall R, Thompson P, Cheadle JP, Ravine D, et al. Renal cystic disease in tuberous sclerosis: role of the polycystic kidney disease 1 gene. *Am J Hum Genet.* 1997;61(4):843-51.

25. Consugar MB, Wong WC, Lundquist PA, Rossetti S, Kubly VJ, Walker DL, et al. Characterization of large rearrangements in autosomal dominant polycystic kidney disease and the PKD1/TSC2 contiguous gene syndrome. *Kidney Int.* 2008;74(11):1468-79.
26. Bissler JJ, Kingswood JC, Radzikowska E, Zonnenberg BA, Frost M, Belousova E, et al. Everolimus for angiomyolipoma associated with tuberous sclerosis complex or sporadic lymphangioleiomyomatosis (EXIST-2): a multicentre, randomised, double-blind, placebo-controlled trial. *Lancet.* 2013;381(9869):817-24.
27. Lam HC, Siroky BJ, and Henske EP. Renal disease in tuberous sclerosis complex: pathogenesis and therapy. *Nat Rev Nephrol.* 2018;14(11):704-16.
28. Wu H, Chen J, Xu J, Dong Z, Meyuhas O, and Chen JK. Blocking rpS6 Phosphorylation Exacerbates Tsc1 Deletion-Induced Kidney Growth. *J Am Soc Nephrol.* 2016;27(4):1145-58.
29. Trudel M, Lanoix J, Barisoni L, Blouin MJ, Desforges M, L'Italien C, et al. C-myc-induced apoptosis in polycystic kidney disease is Bcl-2 and p53 independent. *J Exp Med.* 1997;186(11):1873-84.
30. Parrot C, Kurbegovic A, Yao G, Couillard M, Côté O, and Trudel M. c-Myc is a regulator of the PKD1 gene and PC1-induced pathogenesis. *Hum Mol Genet.* 2019;28(5):751-63.
31. Legouis D, Bataille A, Hertig A, Vandermeersch S, Simon N, Rondeau E, et al. Ex vivo analysis of renal proximal tubular cells. *BMC Cell Biol.* 2015;16:12.
32. Fernando MR, Reyes JL, Iannuzzi J, Leung G, and McKay DM. The pro-inflammatory cytokine, interleukin-6, enhances the polarization of alternatively activated macrophages. *PLoS One.* 2014;9(4):e94188.
33. Wu X, Xu W, Feng X, He Y, Liu X, Gao Y, et al. TNF-a mediated inflammatory macrophage polarization contributes to the pathogenesis of steroid-induced osteonecrosis in mice. *Int J Immunopathol Pharmacol.* 2015;28(3):351-61.
34. Petrovic-Djergovic D, Popovic M, Chittiprol S, Cortado H, Ransom RF, and Partida-Sánchez S. CXCL10 induces the recruitment of monocyte-derived macrophages into kidney, which aggravate puromycin aminonucleoside nephrosis. *Clin Exp Immunol.* 2015;180(2):305-15.
35. Crowther CA, Ashwood P, Andersen CC, Middleton PF, Tran T, Doyle LW, et al. Maternal intramuscular dexamethasone versus betamethasone before preterm birth (ASTEROID): a multicentre, double-blind, randomised controlled trial. *Lancet Child Adolesc Health.* 2019;3(11):769-80.
36. Au KS, Hebert AA, Roach ES, and Northrup H. Complete inactivation of the TSC2 gene leads to formation of hamartomas. *Am J Hum Genet.* 1999;65(6):1790-5.

37. Lam HC, Nijmeh J, and Henske EP. New developments in the genetics and pathogenesis of tumours in tuberous sclerosis complex. *J Pathol.* 2017;241(2):219-25.
38. Hung TH, Hsieh TT, Wu CP, Li MJ, Yeh YL, and Chen SF. Mammalian target of rapamycin signaling is a mechanistic link between increased endoplasmic reticulum stress and autophagy in the placentas of pregnancies complicated by growth restriction. *Placenta.* 2017;60:9-20.
39. Park H, Chang CS, Choi SJ, Oh SY, and Roh CR. Sirolimus therapy for fetal cardiac rhabdomyoma in a pregnant woman with tuberous sclerosis. *Obstet Gynecol Sci.* 2019;62(4):280-4.
40. Anderl S, Freeland M, Kwiatkowski DJ, and Goto J. Therapeutic value of prenatal rapamycin treatment in a mouse brain model of tuberous sclerosis complex. *Hum Mol Genet.* 2011;20(23):4597-604.
41. Colla L, Diena D, Rossetti M, Manzione AM, Marozio L, Benedetto C, et al. Immunosuppression in pregnant women with renal disease: review of the latest evidence in the biologics era. *J Nephrol.* 2018;31(3):361-83.
42. Shah OJ, Anthony JC, Kimball SR, and Jefferson LS. Glucocorticoids oppose translational control by leucine in skeletal muscle. *Am J Physiol Endocrinol Metab.* 2000;279(5):E1185-90.
43. Shah OJ, Kimball SR, and Jefferson LS. Acute attenuation of translation initiation and protein synthesis by glucocorticoids in skeletal muscle. *Am J Physiol Endocrinol Metab.* 2000;278(1):E76-82.
44. Wang H, Kubica N, Ellisen LW, Jefferson LS, and Kimball SR. Dexamethasone represses signaling through the mammalian target of rapamycin in muscle cells by enhancing expression of REDD1. *J Biol Chem.* 2006;281(51):39128-34.
45. Schmidt EV, Ravitz MJ, Chen L, and Lynch M. Growth controls connect: interactions between c-myc and the tuberous sclerosis complex-mTOR pathway. *Cell Cycle.* 2009;8(9):1344-51.
46. Hartleben G, Müller C, Krämer A, Schimmel H, Zidek LM, Dornblut C, et al. Tuberous sclerosis complex is required for tumor maintenance in MYC-driven Burkitt's lymphoma. *EMBO J.* 2018;37(21).
47. Babcock JT, Nguyen HB, He Y, Hendricks JW, Wek RC, and Quilliam LA. Mammalian target of rapamycin complex 1 (mTORC1) enhances bortezomib-induced death in tuberous sclerosis complex (TSC)-null cells by a c-MYC-dependent induction of the unfolded protein response. *J Biol Chem.* 2013;288(22):15687-98.

48. Wu L, Yi B, Wei S, Rao D, He Y, Naik G, et al. Loss of FOXP3 and TSC1 Accelerates Prostate Cancer Progression through Synergistic Transcriptional and Posttranslational Regulation of c-MYC. *Cancer Res.* 2019;79(7):1413-25.
49. Husson H, Manavalan P, Akmaev VR, Russo RJ, Cook B, Richards B, et al. New insights into ADPKD molecular pathways using combination of SAGE and microarray technologies. *Genomics.* 2004;84(3):497-510.
50. Song X, Di Giovanni V, He N, Wang K, Ingram A, Rosenblum ND, et al. Systems biology of autosomal dominant polycystic kidney disease (ADPKD): computational identification of gene expression pathways and integrated regulatory networks. *Hum Mol Genet.* 2009;18(13):2328-43.
51. Zhou X, Fan LX, Peters DJ, Trudel M, Bradner JE, and Li X. Therapeutic targeting of BET bromodomain protein, Brd4, delays cyst growth in ADPKD. *Hum Mol Genet.* 2015;24(14):3982-93.
52. Onda H, Lueck A, Marks PW, Warren HB, and Kwiatkowski DJ. Tsc2(+/-) mice develop tumors in multiple sites that express gelsolin and are influenced by genetic background. *J Clin Invest.* 1999;104(6):687-95.
53. Li Q, Rao R, Vazzana J, Goedegebuure P, Odunsi K, Gillanders W, et al. Regulating mammalian target of rapamycin to tune vaccination-induced CD8(+) T cell responses for tumor immunity. *J Immunol.* 2012;188(7):3080-7.
54. Berezhnoy A, Castro I, Levay A, Malek TR, and Gilboa E. Aptamer-targeted inhibition of mTOR in T cells enhances antitumor immunity. *J Clin Invest.* 2014;124(1):188-97.
55. Chaoul N, Fayolle C, Desrues B, Oberkampf M, Tang A, Ladant D, et al. Rapamycin Impairs Antitumor CD8+ T-cell Responses and Vaccine-Induced Tumor Eradication. *Cancer Res.* 2015;75(16):3279-91.
56. Liu HJ, Lizotte PH, Du H, Speranza MC, Lam HC, Vaughan S, et al. TSC2-deficient tumors have evidence of T cell exhaustion and respond to anti-PD-1/anti-CTLA-4 immunotherapy. *JCI Insight.* 2018;3(8).
57. Liu HJ, Krymskaya VP, and Henske EP. Immunotherapy for Lymphangioleiomyomatosis and Tuberous Sclerosis: Progress and Future Directions. *Chest.* 2019;156(6):1062-7.
58. Swenson-Fields KI, Vivian CJ, Salah SM, Peda JD, Davis BM, van Rooijen N, et al. Macrophages promote polycystic kidney disease progression. *Kidney Int.* 2013;83(5):855-64.
59. Cassini MF, Kakade VR, Kurtz E, Sulkowski P, Glazer P, Torres R, et al. Mcp1 Promotes Macrophage-Dependent Cyst Expansion in Autosomal Dominant Polycystic Kidney Disease. *J Am Soc Nephrol.* 2018;29(10):2471-81.

60. Lee S, Huen S, Nishio H, Nishio S, Lee HK, Choi BS, et al. Distinct macrophage phenotypes contribute to kidney injury and repair. *J Am Soc Nephrol.* 2011;22(2):317-26.

61. Volovelsky O, Cohen G, Kenig A, Wasserman G, Dreazen A, Meyuhas O, et al. Phosphorylation of Ribosomal Protein S6 Mediates Mammalian Target of Rapamycin Complex 1-Induced Parathyroid Cell Proliferation in Secondary Hyperparathyroidism. *J Am Soc Nephrol.* 2016;27(4):1091-101.

Figures

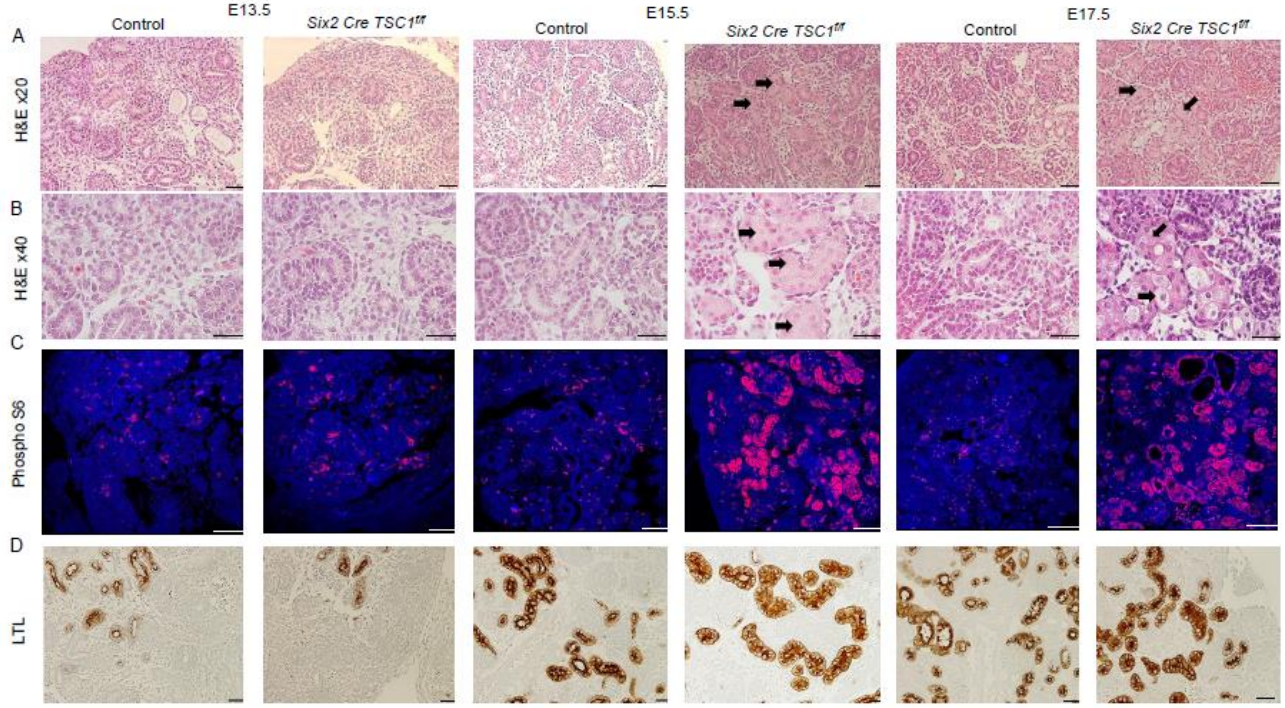

Figure 1. ***TSC1*** **deletion in NPCs is associated with mTOR pathway activation in proximal tubular cells (PTCs).** Kidney sections at different embryonic ages as indicated were stained with (A) H&E, (B) enlarged kidney sections as in A. (C) phosphorylated S6 analyzed by IF. (D) LTL antibody by IHC. Scale bar = 50 µm, n=3. Black arrows indicate the injured PTCs with swollen appearance and occluded lumen.

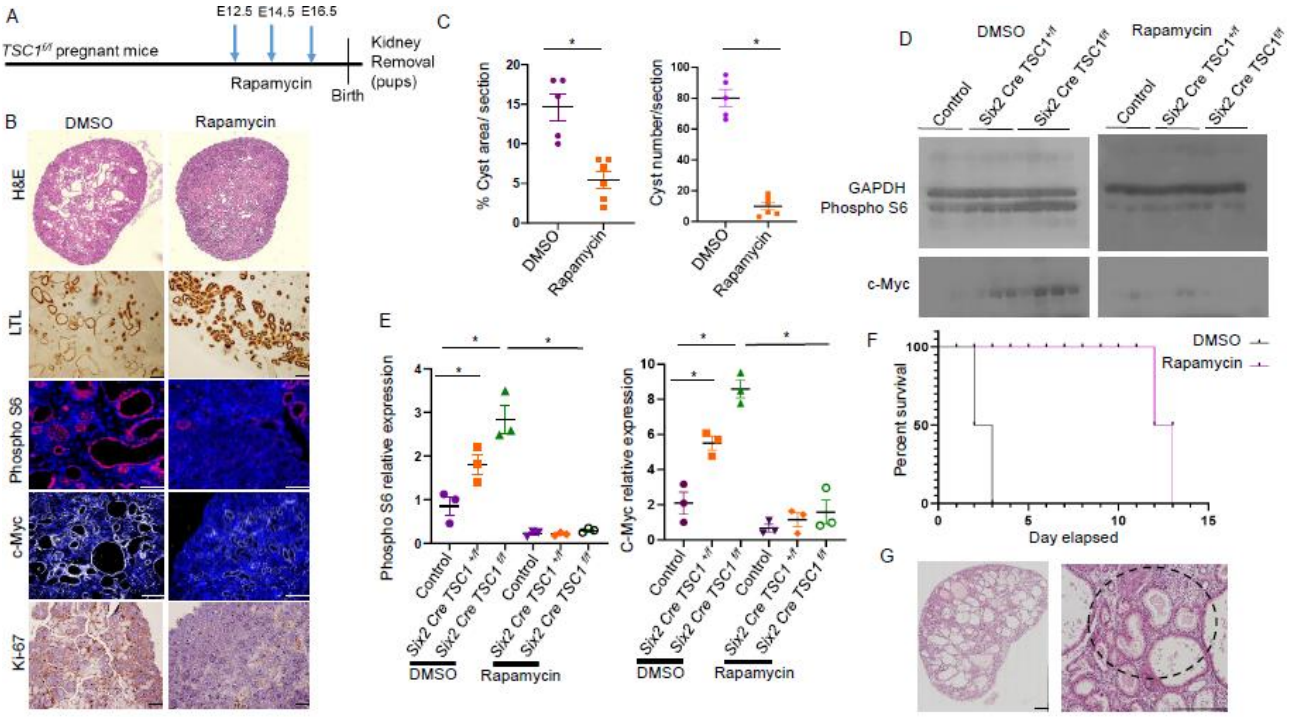

Figure 2. **mTOR inhibition by rapamycin prevents proximal tubular damage and cyst formation and prolongs survival of *Six2 Cre* $^{tg/+}$*TSC1*$^{f/f}$ mice.** (A) Experimental time course**.** *TSC1*$^{f/f}$ females were mated with *Six2 Cre* $^{tg/+}$*TSC1*$^{f/+}$ males. Rapamycin or vehicle (DMSO) were injected at the indicated gestational ages. Kidneys of *Six2 Cre* $^{tg/+}$*TSC1*$^{f/f}$ P0 pups were removed. (B) Renal sections from *Six2 Cre TSC1*$^{f/f}$ mice were stained by H&E, IHC for LTL and Ki-67 and IF for phospho S6 (pS6) and c-Myc. Scale bar = 50µm. n=3 in each group. (C) Quantitative analysis of cyst area and number of cyst per section as in B .*, P<0.05, compared to vehicle, DMSO, n=5; rapamycin, n=6 (D) Western blots of kidney extracts from control, *Six2 Cre TSC1*$^{f/+}$, *Six2 Cre TSC1*$^{f/f}$ mice treated with rapamycin or vehicle as in A, analyzed for pS6, GAPDH and c-Myc, showing elevated pS6 and c-Myc expression in heterozygous and homozygous renal extracts compared to control and reduction in the expression of these proteins upon rapamycin treatment (E) Quantification of the Western blot as in D. *, P<0.05, compared to control (WT), n=3 in each group. (F) Kaplan-Meier curve showing improved survival rate of rapamycin-treated *Six2 Cre* $^{tg/+}$*TSC1*$^{f/f}$ mice (n=6), compared to DMSO (n=6). (**G**) H&E staining of P14 offspring of rapamycin-treated *Six2 Cre* $^{tg/+}$*TSC1*$^{f/f}$ mice as in A, demonstrating mononuclear infiltrate. The dashed circle indicates mononuclear inflammation site. Scale bar = 500µm, (n=3). Unpaired t-test was used for C and one-way ANOVA statistical analysis was used followed by Duncan's post-hoc test for E.

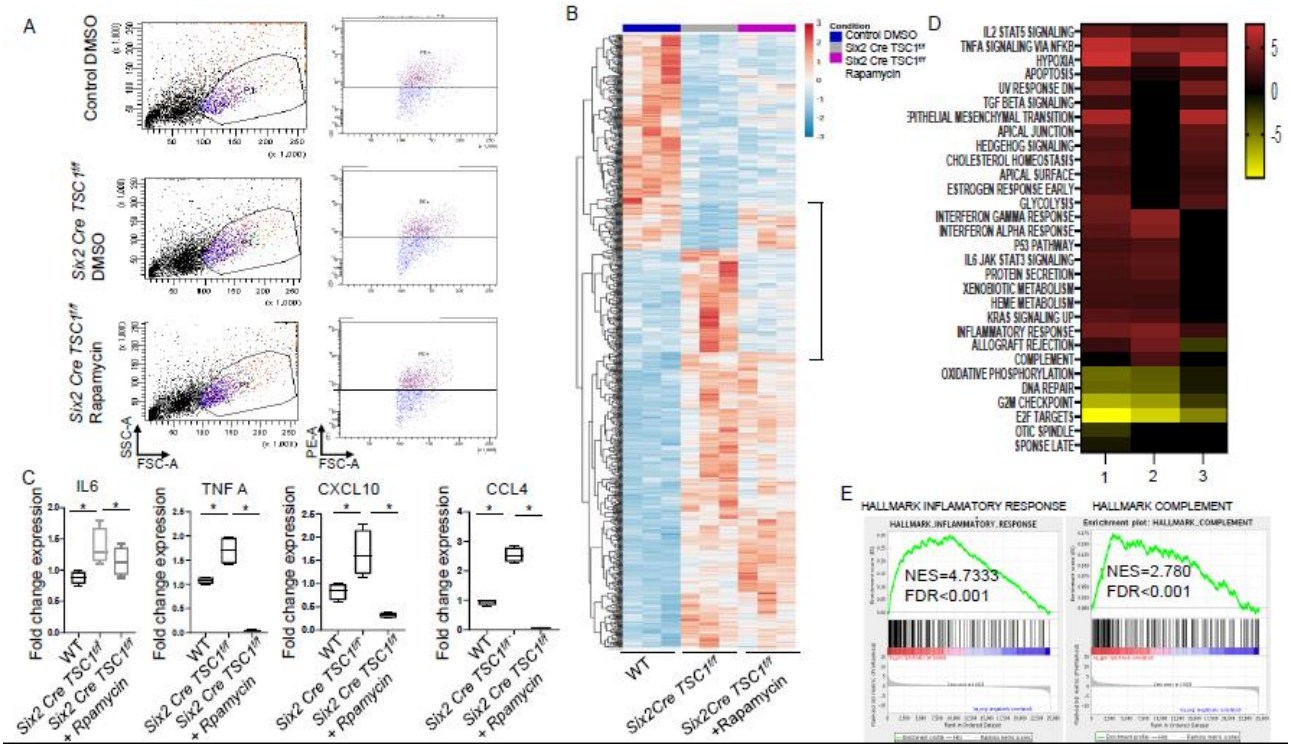

Figure 3. ***TSC1* deletion alters the expression of genes associated with inflammation in embryo renal proximal tubule cells (PTCs) and this is reversed by rapamycin treatment during pregnancy.** (A) Kidneys from E18.5 control and *TSC1* null mice with and without rapamycin, given as in Figure 2A, were removed, cells dissociated and proximal tubule cells stained with PE-conjugated prominin-1 antibody. Prominin-1-positive cells were monitored and sorted by FACS to isolate PTCs. Representative analyses of 3 samples for each group. (B) Heatmap visualization showing relative gene expression in sorted PTCs from control and *Six2 Cre TSC1 $^{f/f}$* embryos without (DMSO) and with rapamycin given during pregnancy. n=3 for each group. (C) Validation by qRT-PCR of changes in expression of genes that are associated with inflammatory response and macrophage polarization, that were chosen based on B and C. In each group n=4. One-way ANOVA statistical analysis was used followed by Duncan's post-hoc test. *, P<0.05. (D) Heat map of potential pathways affected by TSC1 deletion and the effect of rapamycin treatment on these pathways in PTCs. The changes in pathways were calculated according to the gene set enrichment analysis (GSEA) in B. 1- The ratio between *Six2 Cre TSC1$^{f/f}$* PTCs treated with rapamycin vs WT PTC treated with DMSO. 2- The ratio between *Six2 Cre TSC1$^{f/f}$* PTCs treated with DMSO vs WT PTCs with DMSO. 3- The ratio between *Six2 Cre TSC1$^{f/f}$* PTCs treated with rapamycin vs *Six2 Cre TSC1$^{f/f}$* PTC with DMSO. (E) GSEA analysis of the inflammatory response and complement pathways in *Six2 Cre TSC1$^{f/f}$* PTCs compared to control WT PTCs.

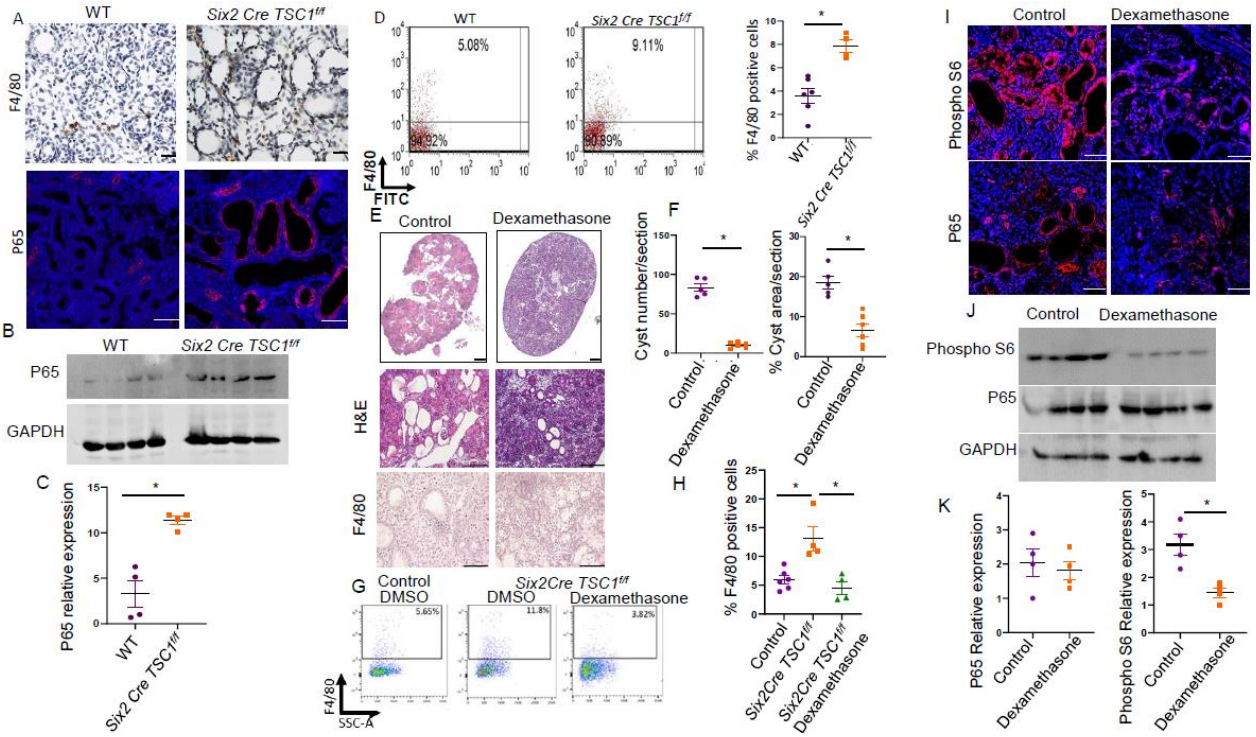

Figure 4. **Dexamethasone administered during pregnancy reduces cyst formation and mTORC1 activity in TSC mice.** (A) Renal sections of control and *Six2 Cre* $^{tg/+}$*TSC1*$^{f/f}$ mice (P0) were stained with anti F4/80 marker (macrophages) and anti NFkB P65. Scale bar = 50 µm, n=3. (B) Western blot for P65 and control GAPDH in homogenized kidneys from control and *TSC1* KO mice. (C) Quantification of the Western blot in B. *, p<0.05, n=4. (D) Kidneys from mice as in A were removed. Cells were dissociated and proximal tubule cells stained with APC- conjugated F4/80. The percentage of F4/80^{+} cells was determined by FACS. WT, n=6, *Six2 Cre TSC1*$^{f/f}$, n=4. (E) Representative H&E staining of kidney sections from dexamethasone and control (PBS), treated *Six2 Cre* $^{tg/+}$*TSC1*$^{f/f}$ mice, showing reduced cyst formation after dexamethasone. Scale bar=500 µm. (F) Quantification of the cyst area and number per section in the different groups as in F. dexamethasone (n=6) and control (n=5), *, p<0.05. (G) Representative FACS analysis. Kidneys of WT, *Six2 Cre TSC1*$^{f/f}$ treated with either PBS or dexamethasone as indicated, were dissociated and stained with APC- conjugated F4/80 and subjected to FACS analysis. (H) Quantification of the percentage of F4/80^{+} cells in each group as in G. WT n=5, *Six2 Cre TSC1* $^{f/f}$ with PBS n=4 and *Six2 Cre TSC1* $^{f/f}$ treated with dexamethasone n=4. (I) Sections as in E were stained for pS6 and P65. Scale bar = 50 µm, n=3. (J) Kidneys were homogenized as in E and the expression of P65, pS6 and GAPDH were analyzed by Western blots n=4. (K) Quantification of the Western blots as shown in J. *, P<0.05. Unpaired t-test was used for C, D, F and K and one-way ANOVA statistical analysis was used followed by Duncan's post-hoc test for H.

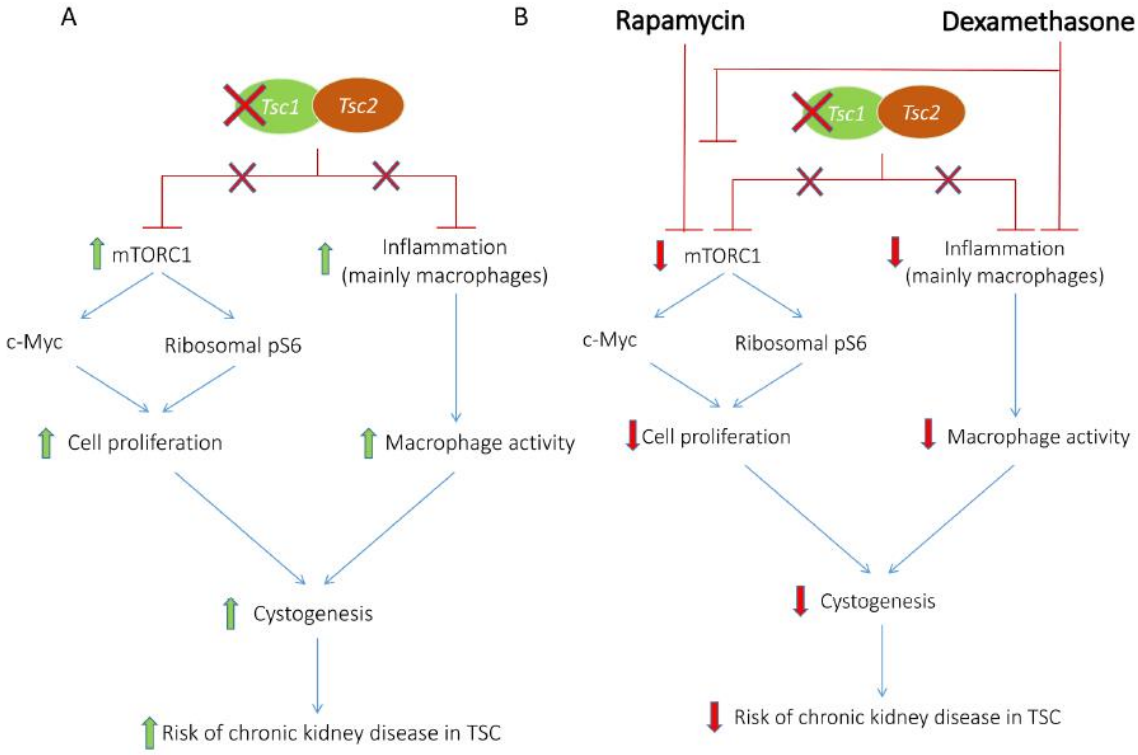

Figure 5. **Scheme summarizing the proposed mechanism by which rapamycin and dexamethasone administration during pregnancy prevent cystic kidney disease in TSC.** TSC1 deletion in nephron progenitor cells leads to increased mTORC1 activity and an inflammatory response in the nephron. Cysts arise from proximal tubular cells in the developing nephrons as a result of high cell proliferation rate and macrophage activity which increase the risk of CKD in adult TSC patients. By reducing mTORC1 activity, rapamycin leads to decreased ribosomal translation and c-Myc expression, thereby decreasing the proliferation rate of the tubular cells. Dexamethasone ameliorates cyst formation by inhibiting both mTORC1 and the inflammatory response in the cysts.